promoting access to White Rose research papers

Universities of Leeds, Sheffield and York
http://eprints.whiterose.ac.uk/

This is an author produced version of a paper published in **Composites Part A-Applied Science and Manufacturing**.

White Rose Research Online URL for this paper:
http://eprints.whiterose.ac.uk/43690

Published paper

Johnson, A.C., Hayes, S.A., Jones, F.R. (2012) *The role of matrix cracks and fibre/matrix debonding on the stress transfer between fibre and matrix in a single fibre fragmentation test*, Composites Part A- Applied Science and Manufacturing, 43 (1), pp. 65-72

http://dx.doi.org/10.1016/j.compositesa.2011.09.005

White Rose Research Online
eprints@whiterose.ac.uk

The role of matrix cracks and fibre/matrix debonding on the stress transfer between fibre and matrix in a single fibre fragmentation test

Anbu Clemensis Johnson[a,b], Simon A. Hayes[a] & Frank R. Jones[a]*

[a]Department of Materials Science and Engineering, University of Sheffield, Sir Robert Hadfield Building, Mappin Street, Sheffield, S1 3JD, U.K.

[b]Department of Mechanical and Industrial Engineering, Caledonian College of Engineering, P.O.Box: 2322, CPO Seeb 111, Sultanate of Oman.

Abstract

The single fibre fragmentation test is commonly used to characterise the fibre/matrix interface. During fragmentation, the stored energy is released resulting in matrix cracking and/or fibre/matrix debonding.

Axisymmetric finite element models were formulated to study the impact of matrix cracks and fibre/matrix debonding on the effective stress transfer efficiency (EST) and stress transfer length (STL). At high strains, plastic deformation in the matrix dominated the stress transfer mechanism. The combination of matrix cracking and plasticity reduced the EST and increased STL.

For experimental validation, three resins were formulated and the fragmentation of an unsized and uncoupled E-glass fibre examined as a function of matrix properties. Fibre failure was always accompanied by matrix cracking and debonding. With the stiff resin, debonding, transverse matrix cracking and conical crack initiation were observed. With a lower modulus and lower yield strength resin the transverse matrix crack length decreased while that of the conical crack increased.

Keywords: Matrix cracking, transverse matrix crack, finite element analysis, stress transfer, single fibre composite, fragmentation test, glass fibre.

---

*Corresponding author. Tel.: +44-114-222-5477; Fax: +44-114-222-5943.

E-mail: f.r.jones@sheffield.ac.uk (F.R. Jones).

1. Introduction

The fragmentation test is a commonly used test method for the characterization of the fibre/matrix interface. It displays the basic phenomena that are present in multi-fibre composites such as fibre fracture, interfacial debonding, matrix yielding and matrix cracking [1]. In the fragmentation test a continuous fibre is embedded in a resin coupon and subjected to axial tension. Load transfer from matrix to fibre occurs through interfacial shear. As the load increases the fibre breaks into smaller and smaller fragments until they are too short to be further loaded to fracture. Kelly and Tyson [2] related the interfacial shear stress τ to the critical fibre length l_c in the following equation (1),

$$\tau = \frac{r\sigma_{uf}}{l_c} \tag{1}$$

where r is the radius of the fibre and σ_{uf} is the strength of the fibre at a length l_c.

Equation (1) assumes that a constant shear stress exists at the interface of the fragment. This assumption is valid when fragmentation has saturated, either as a result of complete debonding or matrix yielding at the interface.

In the fragmentation test a fibre-break is often accompanied by debonding and/or matrix cracking. Three failure modes are encountered; a transverse matrix crack, an inclined conical matrix crack and/or fibre/matrix debond [3, 4]. The failure mode depends on the quality of interface [4] as indicated below;

(a) If the interface is strong in an elastic matrix, a fibre-break is accompanied by a transverse matrix crack.
(b) If the interface bond strength is good but the matrix has a low shear strength an inclined conical crack will form.
(c) Where the interface bond strength is low, debonding is initiated at the interface.

The matrix mechanical properties also have a significant influence on the formation of the matrix cracks. However, the reason for the formation of transverse or conical

matrix cracks is a subject of further study. According to Huang and Talreja [5] plastic deformation precedes the fracture and the predictive finite element model uses critical plastic strain as a criterion for facture initiation of conical matrix crack.

During a fibre-break the stored elastic energy is released to the surrounding matrix causing either interface failure and/or matrix cracking. Studies by various authors [3, 4, 6, 7] have shown that matrix cracks propagate with applied strain, perpendicular to the fibre fracture. Matrix cracks which form at lower applied strains propagate a shorter distance into the polymer than those which form at high strains, because of a lower stored elastic energy [7]. It was also shown that transverse matrix cracks propagate faster than conical matrix cracks which are usually at 45^o to the fibre axis [4]. The existence of a matrix crack changes the stress field surrounding the fibre-break and influences the stress transfer across the interface. An analytical and finite element study by Liu et al. [8, 9] has shown that a matrix crack significantly affects the rate of stress transfer. A matrix crack emanating from a fibre-break can cause premature failure of a high volume fraction composite because the stress concentration on adjacent fibres and matrix leads to the formation a crack of critical dimensions which propagates through the composite. Thus the fibres do not reach their full load carrying potential [4]. Recently Behzadi et al. [10] have studied the role of multiple fibre-breaks on the failure of a 0^o fibre composite. It has been reported that the formation of a matrix crack is influenced by cure temperature, matrix modulus, surface treatment of the fibres, and strain rate [3, 4, 11-13].

An energy based approach is frequently used to characterise the interface by balancing the stored energy in the system to that released in the formation of new debonded surfaces. Energy employed in the formation of a matrix crack should also be included to correctly characterise the interface. Strain energy released by interfacial debonding was estimated to be 57–342 J/m^2 and for conical and transverse matrix cracks 58–103 J/m^2 [3]. Therefore the force required to initiate debonding appears to be larger than that for matrix cracking.

In the present work, a systematic experimental study was performed to understand the influence of matrix modulus and yield strength on the formation of a matrix crack and/or fibre/matrix debonding. Following this finite element analysis was used to

study the impact of transverse matrix cracks, conical matrix cracks and fibre/matrix debonding on the stress transfer efficiency at the fibre/matrix interface since there is no established method for quantifying the stress in glass and other fibres where direct methods such as laser Raman spectroscopy, which can be used for high modulus carbon and ceramic (eg alumina) fibres, cannot be employed.

2. Experimental

2.1. Fibres

The unsized E-glass fibres used in this work were obtained from Owens Corning Fiberglass, with a fibre diameter of 15.32 ± 0.46 μm.

2.2. Matrix resin

The epoxy resin used was Araldite LY 5052 and GY 298 (Ciba-Geigy). These were mixed in proportions of 100/0 (PHY), 70/30 (PMY) and 60/40 (PLY) with the calculated amount of hardener Aradur 5052 to give three different resin types. This ensured that the resins were chemically similar but with varying mechanical properties. The proportions used are given in Table 1. Properties of the elastic resin used were taken from reference 13. 'P' denotes plastic, 'E' denotes elastic, H, M, L stands for high, medium, low and 'Y' denotes yield strength. The resins were blended using a mechanical stirrer for 5 minutes and degassed in a vacuum chamber.

For the preparation of fragmentation test specimens, single untreated-unsized E-glass fibres were separated from the fibre tow and mounted across a metal frame. The mounted fibres were then carefully placed in the dog-bone mould and the degassed resin was poured into the dog-bone moulds and cured in an oven at 80^{o} C for 8 hours. The resin properties are referred here as,

PHY = High modulus and high yield strength epoxy resin

PMY = Medium modulus and medium yield strength epoxy resin

PLY = Low modulus and low yield strength epoxy resin

EH = Elastic high modulus resin

EL = Elastic low modulus resin

2.3. Specimen testing (single fibre fragmentation test)

Testing of the single fibre dog-bone specimens was performed using a specially designed mini-tensile testing machine supplied by Micromaterials Ltd, Wrexham, U.K. The set-up is illustrated schematically in Figure 1(a). Testing of the single fibre dog bone samples were carried out by clamping the specimens within the grips of the testing machine, and loading the samples at a crosshead speed of 0.13 mm min^{-1}, with the use of the stepper motor. The output from the load cell, and the LVDT (linear voltage displacement transducer) were monitored using a commercial data-logging package (PICOLOG), which enabled direct observation of stress and strain applied to the sample. The fragmentation test was also monitored using a transmitted optical light microscope interfaced to a JVC CCD camera (the CCD was connected to an external monitor and the computer). A polarising plate was affixed to the end of the microscope, and another polarising plate (out of phase) was affixed on top of the light source. This enabled any stress birefringence phenomena occurring within the sample to be observed simultaneously on the screen (Figure 1(b)). The strain applied to the specimens was determined by measuring the distance between the lines before and after the application of load. The monitored length was 20 mm along the gauge length. This was achieved by measuring the sample using a vernier caliper fitted to the microscope. Once the required length was obtained the test was interrupted and the specimen was removed for further study. A custom-written computer program (IMAGE) windows based C++ program was used to quantify the images captured during the single fibre fragmentation test. For each specific study three specimens were examined.

3. FEA modelling

The axisymmetric finite element model given in Figure 2, was used to study five representative micromechanical events which were observed during fragmentation of a single embedded filament. The material properties used for modelling were extracted from the experimental data. Five cases were modelled:

(1) A perfectly bonded fibre and matrix (PB)

(2) Perfectly bonded fibre with a two fibre diameter-transverse matrix crack (PBTC)
(3) Perfectly bonded fibre with two fibre diameter inclined-conical matrix crack (PBCC)
(4) Two fibre diameter debond (DB)
(5) Two fibre diameter debond with transverse matrix crack (DBTC)

The model was 0.5 mm in length and 0.3 mm in width from the centre of the fibre. The dimensions were selected in order to reduce the edge effects. The fibre was assumed to be elastic and the matrix elastic or elasto-plastic. Fibre and matrix were assumed to be two cylinders with the fibre cylinder inside the matrix cylinder (Figure 2). The following boundary conditions were applied to the FEM,

- AB was constrained with displacement U_x=0
- BC was constrained with displacement U_y=0
- DC free surface
- Incremental displacement was applied along AD in the Y direction

A fibre-break was introduced by eliminating a single row of elements by using the ANSYS 5.6.1. 'ekill' command. This reduced the mechanical properties of those elements by a factor of $1x10^{-6}$. A transverse matrix crack was modelled by releasing the appropriate displacement boundary conditions along the side AD. An inclined conical crack was simulated by introducing a discontinuity of 0.03 mm in the matrix elements which were at 45º to the fibre axis by using duplicate nodes along EF (Figure 3 (b)). The same method was used to model interfacial debonding with a discontinuity of 0.03 mm between the fibre and matrix.

Plane 182-2-D-Structural Solid four node elements were used for all the models. In the case of the simulation of a debonded interface, Targe169 and Conta172-2-D-3-Node Surface to Surface contact element pairs were used (the region shown as 'g' in Figure 3 (a)). These elements satisfy the Coulomb friction law as defined by equation (2).

$$\tau_{\lim} = \mu P + b \tag{2}$$

where, τ_{lim} is the limiting shear stress (shear stress beyond which the elements slide with respect to each other); τ is the equivalent shear stress (shear stress developed at the contact surface); μ is the friction coefficient; P is the contact normal pressure and

b is the contact cohesion. When the equivalent shear stress exceeds τ_{lim}, the contact and the target surfaces slide relative to each other.

The number of elements used in the finite element model varied from model to model but on average was greater than 16000 elements. The FEA mesh was graduated such as to maximise the computational effort close to the tips of the fibre and matrix cracks where the maximum stress concentration existed and yielding took place. The mechanical properties used in the modelling are given in Table 2.

4. Results

4.1. Experimental study of single fibre fragmentation test

Single fibre fragmentation was conducted using three matrix resins whose properties are given in Table 2. A gauge length of 20 mm was fixed. Separate specimens were used for different strain levels. This made it convenient for the accurate measurement of the lengths of debonds and transverse matrix cracks, at each level of strain. The fracture patterns observed during the fragmentation test at 6 % applied strain is presented in Figure 4.

The fracture patterns were mainly dependent on the matrix system used. The strain for onset of fibre fracture was slightly greater than 3 % which depended on the strength of the fibre filaments. In all three resin systems, fibre/matrix debonding and transverse matrix cracking were observed. The extent of fibre/matrix debonding and transverse matrix cracking was found to be different for the PHY and PMY resin systems. It was observed that the transverse matrix cracks were larger in the PHY resin system with very small conical cracks. This is because the energy absorbing capability of the PHY resin is less compared to PMY and PLY resin systems. It also suggests that the rate of crack growth is higher for stiff brittle resin systems. In the case of PMY resin the length of transverse matrix cracks was reduced with an increase in the size of conical matrix cracks. The increase is further accelerated in the case of PLY resin where the transverse crack length decreases further. It seems that the energy used in the formation of a transverse crack is transferred to the formation of conical matrix cracks

as the yield strength of the resin decreases. Another important observation was the transverse matrix crack formed on both sides of the filament as shown in Figure 4(d) were not symmetrical as shown by earlier authors [4, 7]. Using an optical microscope the length of transverse matrix crack and debonded length along the fibre/matrix interface at each fibre-break were measured for each fragment and presented in Table 3.

From Table 3 it can be seen that the lengths of the transverse matrix cracks and debonds increased with applied strain. In the case of a glass fibre in the PLY resin system the debonded length appears to remain approximately constant, without an observable significant increase with strain.

4.2. Finite element study of single fibre fragmentation test

Observations from the fragmentation test revealed the existence of an apparent mixed-mode failure mechanism involving fibre/matrix debonding and matrix cracking. The finite element model was formulated to study the influence of debonding and matrix cracking on the effective stress transfer and stress transfer length. Effective stress transfer efficiency (EST) in % is defined as the maximum axial stress attained in the fibre centre divided by the theoretical maximum achievable under elastic conditions (Young's modulus of fibre × applied strain). Stress transfer length (STL) is defined by the point at which the stress in the fibre reaches 90 % of the maximum axial stress in the fibre [14].

4.2.1. Influence of a matrix crack on effective stress transfer efficiency (EST)

The calculated results of EST for a perfectly bonded glass fibre in the different resin systems with and without transverse matrix crack are shown Figure 5. It can be seen that the stress transfer characteristics varies with the modulus and yield strength of the resin system. The highest modulus elastic matrix has the maximum value of EST. The EST also remains constant for the elastic system at increasing strain levels. In the case of the plastic matrices it can be observed that EST decreases and is more rapid for the low modulus low yield strength matrix. The differing degrees of stress transfer in the presence of a fibre-break with transverse cracking are discussed in Section 5.

Figure 6 shows that the stress transfer efficiency is maximum for the perfectly bonded fibre and decreases with the introduction of transverse and conical matrix crack. The difference between the stress transferred back to the fibres at a fibre-break with a conical matrix crack was found to be minimal. The interesting point worth noting is ,that the debonded fibre had a higher value of EST. This suggests that limited amount of debonding at the fibre ends can decrease the occurrence and extent of matrix cracking. In this case, interfacial debonding is found to be more beneficial in transferring stress to the fibre. However, in the case where both matrix cracks and fibre/matrix debonding co-exists, the stress transfer efficiency further decreases.

In the case where the fibre is in a low modulus matrix with low yield strength, the stress transfer efficiency for the debonded fibre falls below that of the case for a matrix crack as shown in Figure 7. This contrasting behaviour is due to the plastic properties of the low modulus matrix with low yield strength. These effects sharply decrease the stress transfer capability of the PLY resin.

4.2.2. Influence of matrix crack on stress transfer length (STL)

Stress transfer lengths were calculated from the axial stress profile for different experimental conditions studied and presented in Table 4. The elastic matrices tend to have a constant STL value whereas for plastic matrices it increases gradually with applied strain. In the perfectly bonded case STL increased linearly for PHY and PLY resin systems. With the inclusion of a transverse matrix crack STL tends to further increase. For the elastic resins it almost doubles and for PHY and PLY resin system it increased by about 10 and 20 %, respectively. This suggests that the presence of matrix crack has significant effect on stress transfer.

It can also be seen for a perfectly bonded fibre (PB) that the STL for EH is about 0.062 mm and 0.16 mm for EL. This shows that the effectiveness of stress transfer to the fibre is lower for more compliant matrix. On considering the PHY resin system in Table 4, it was expected that the perfectly bonded fibre would have the lowest value. However, it is interesting to note that the STL for a debonded fibre (DB) is less than that for the case of a transverse matrix crack (DBTC) up to a strain of 1.5 %. In the

case of DBTC the STL is higher than other studied cases. The STL of PHY and PLY systems with debonded fibres cross the lines for the PBTC and PBCC systems before 1% strain is reached. This is due the influence of matrix plasticity.

5. Discussion

Fibre fracture occurs when the maximum fibre axial stress reaches the fibre tensile strength resulting in fibre/matrix debonding and/or matrix cracking. The matrix cracks formed at low applied strains are small. This is because fibre facture at low strains are a result of fibre flaws or weak points in the fibre where the dissipation of the lower stored energy limits the size of the resin cracks [7]. Cracks initiated at higher strains are generally larger due to the dissipation of more energy. Mixed failure mode is characterised by the presence of transverse matrix cracks, conical matrix cracks and fibre/matrix debonding. The transverse matrix crack is noticeably larger due to the brittle nature of the matrix (Figure 4(a)). Initiation of a conical matrix crack is attributed to plastic deformation of the matrix and debonding is characteristic of unsized glass fibres. When the fibre/matrix bond strength is less than the stresses around the fibre-break, debonding is initiated. Matrix yield strength and stiffness play a significant role in the energy dissipation process and the type of fracture. The lower modulus and lower yield strength of the matrix reduces the length of the transverse matrix crack and increases the length of the conical matrix crack (Figure 4(e)). It also has a higher energy absorbing capability. This explains why the crack growth is smaller for the lower modulus/lower yield strength resin as shown in Table 3. This suggests that by decreasing the modulus and yield strength of the matrix, it is possible to reduce the probability of the formation of a transverse matrix crack and increase the fracture toughness of the composite. However, this results in decreasing the stiffness of the composite.

Since the matrix material was chemically similar with no treatment applied to the fibre it is assumed that the interface was similar for all the three matrix system under study. A noticeable feature in Table 3 is the large scatter in the debonded length data at 4 and 5 % strains. An element of scatter is possible in the measured lengths since we only measured the lengths of the transverse matrix cracks and debonded interface. Formation of conical matrix cracks and the combination of failure modes will influence the extent of transverse matrix cracking and debonding. Some variations in

the data due to the distributions of flaws in the fibres and the variation in fibre diameter are expected.

Since matrix cracks appear following fibre fracture, a greater applied stress is required for a new fibre-break. From Figure 5 it can be seen that the modulus and yield strength of the matrix had a significant influence on the values of EST. The stress transfer ability of the stiffer resin (EH) is higher than the lower modulus resin (EL). The EH system with a higher ratio of matrix to fibre modulus had a higher EST than the EL system which had a lower matrix to fibre modulus ratio. This suggests that for a uniform applied stress, a stiffer material can transfer stress more effectively thereby reducing the ineffective length of a filament. The inclusion of a transverse matrix crack however decreased the effective stress transfer and the stress carrying ability of the fibre. The difference in the case of the EH system was less than 0.5 % but in the case of EL it was about 2.2 %. With PHY and PLY systems, the values of EST show a decreasing trend but the PLY system was more sensitive to the presence of a matrix crack. This effect is predominantly due to matrix plasticity. It can be seen from Figures 6 and 7 how the various failure modes, which are observed during filament fracture in a composite, influence EST. The results of this study indicate that the reinforcing efficiency of a fibre decreases in the presence of matrix cracks, as reported elsewhere [8, 9, 13]. Fibre/matrix debonding with or without matrix cracking further decreases the reinforcing efficiency. An interesting observation was that in the case of the PHY resin, a debonded fibre appears to have a higher value of EST compared to the mixed mode failures in which a matrix crack forms. In contrast, in the presence of the PLY resin the reinforcing efficiency of a debonded fragment depends on the applied strain and falls below the cases with matrix cracks at strains of >1%. This effect is due to matrix plasticity and its importance has been discussed by Tripathi et al. [15]. At low applied strains the stress transfer in the vicinity of the fibre is largely elastic and only a small degree of plasticity may occur at the fibre tip. As the applied strain increases the length of the fibre required to transfer the same level of stress also increases as shown in Table 4. The Finite Element Analysis used a von Mises yield criterion to describe the deformation behaviour of the element at the fibre/matrix interface. However, in the case of an idealized perfectly elastic matrix, a small debond length does not influence significantly EST and STL as shown in Figure 8 and Table 4. Thus a short stress transfer length is required for efficient and uniform loading of

the fibre [16]. From Table 4 it can be seen that the STL values are more or less similar for PBTC and PBCC. This suggests that length of the matrix crack has a greater influence on the maximum stress carrying capability of the fibre. This stress carrying capability of the fibre is further decreased with the coexistence of debonding with matrix cracks.

6. Conclusion

The fragmentation of a single glass fibre in matrices of varying modulus and yield strength has been studied experimentally. The fragmentation test simulates the behaviour of fibres within a 0^0 unidirectional ply or composite so that the observation of matrix cracking and fibre/matrix debonding, which significantly change the ineffective length of the individual fibres, is important in the modelling of the failure criteria.

The following observations were made during the fragmentation test:

- Transverse matrix cracks were larger in the case of a high modulus, high yield strength resin because of the brittle nature of the matrix.
- Conical matrix cracks were found to be longer as the modulus and yield strength of the resin decreased because of lower shear strength of matrix.
- The growth of a conical matrix crack reduced the probability of the formation of a transverse matrix crack.
- Matrix cracks formed on either side of the fibre were not always symmetrical.

These micromechanical observations were modelled using finite element analysis. The influence of matrix modulus and yield strength and the different failure modes, such as transverse matrix cracking, conical matrix cracking and fibre/matrix debonding on the effective stress transfer and the stress transfer length were studied. It was found that the matrix modulus and matrix plasticity significantly influenced the stress transfer efficiency. The initiation of matrix cracking further decreased the reinforcing efficiency of the fibre. The FEA models enabled the effects to be quantified in terms of the stress transfer length (STL) and effective stress transfer efficiency (EST).

Acknowledgements

Dr. Anbu Clemensis Johnson wishes to acknowledge the UK EPSRC (Engineering and Physical Sciences Research Council) for financial support.

References

1. Feillard P, Désarmot G, Favre JP. Theoretical aspects of the fragmentation test. Comp Sci Technol 1994;50:265-79.

2. Kelly A, Tyson WR. Tensile properties of fibre reinforced metals: copper/tungsten and copper/molybdenum. J Mech Phys Solid 1965;13:329-50.

3. Pegoretti A, Accorsi ML, Dibenedetto AT. Fracture toughness of the fibre-matrix interface in glass-epoxy composites. J Mater Sci 1996;31:6145-53.

4. Mullin J, Berry JM, Gatti A. Some fundamental fracture mechanisms applicable to advanced filament reinforced composites. J Comp Mater 1968;2:82-103.

5. Huang H, Talreja R. Numerical simulation of matrix micro-cracking in short fiber reinforced polymer composite: Initiation and propagation. Comp Sci Technol 2006;66:2743-57.

6. Netravali AN, Schwartz P, Phoenix SL. Study of interfaces of high performance glass fibres and DGEBA-based epoxy resins using single-fibre-composite test. Poly Comp 1989;10:385-88.

7. Baillie C, Buxton A. A quantitative study of matrix crack propagation in the fragmentation test. Composites A 1998;29A:1091-97.

8. Liu HY, Mai YW, Ye L, Zhou LM. Stress transfer in the fibre fragmentation test Part III Effect of matrix cracking and interface debonding. J Mater Sci 1997;32:633-41.

9. Liu HY, Mai YW, Ye L. Finite element analysis of stress distribution in a fibre/matrix fragment. Key Eng Mater 1998;145-149:613-20.

10. Behzadi S, Curtis P.T, Jones F.R. Improving the prediction of tensile failure in unidirectional fibre composites by introducing matrix shear yielding Compos Sci Technol 2009;69(14):2421-2427

11. Buxton A, Baillie C. A study of the influence of the environment on the measurement of interfacial properties of carbon fibre/epoxy resin composites. Comp 1994;25:604-08.

12. Detassis M, Pegoretti A, Migliaresi C. Effect of temperature and strain rate on interfacial shear stress transfer in carbon/epoxy model composites. Comp Sci Technol 1995;53:39-46.

13. Johnson AC, Zhao FM, Hayes SA, Jones FR. Influence of a matrix crack on stress transfer to an α-alumina fibre in epoxy resin using FEA and photoelasticity. Comp Sci Technol 2006;66:2023-29.

14. Jacobs E, Verpoest I. Finite element modelling of damage development during longitudinal tensile loading of coated fibre composites. Composites A 1998;29A:1007-12.

15. Tripathi D, Chen F, Jones FR. The effect of matrix plasticity on the stress fields in a single filament composite and the value of interfacial shear strength obtained from the fragmentation test. Proc Roy Soc A: Math Phys Sci 1996;452: 621-53.

16. Johnson AC, Hayes SA, Jones FR. An improved model including plasticity for the prediction of the stress in fibres with an interface/interphase region. Composites A 2005;36:263-71.

Table Captions

Table 1. Resin formulations used in the study.

Table 2. The mechanical properties of the fibres and matrix employed in the Finite Element Model (FEA).

Table 3. Fragmentation test data as a function of matrix properties and applied strain in terms of the number of fragments, transverse matrix crack length (TC) and debond (DB) length. PHY, PMY and PLY refer to epoxy resins with high, medium and low modulus and yield strengths.

Table 4. Stress transfer lengths at different applied strain, obtained from the FEA simulations in the presence of different failure modes and matrix properties.

Resin (pbw)	PH	PM	PL
Araldite LY 5052 (Epoxy 1)	100	70	60
Araldite GY 298 (Epoxy 2)	0	30	40
Aradur 5052 (Hardener)	38	30.57	28.09

pbw – parts by weight

Tab. 1

Property	Fibre	Matrix				
		PHY	PMY	PLY	EH†	EL†
Young's modulus (GPa)	76	2.46	2.38	2.10	5.67	1.39
Poisson's ratio	0.22	0.35	0.35	0.35	0.31	0.36
Tensile yield strength (MPa)	-	79.4	64.7	43.7	-	-
Cold draw strength (MPa)	-	79.3	64.6	43.6	-	-
Diameter of the fibre (mm)	0.015	-	-	-	-	-
Length of the fragment (mm)	1	-	-	-	-	-
Interface friction coefficient, μ	0.2	-	-	-	-	-

†Reference 16

Tab. 2

Strain (%)	Matrix								
	PHY			PMY			PLY		
	Avg. No. of fragments	Avg. TC Length, µm	Avg. DB Length, µm	Avg. No. of fragments	Avg. TC Length, µm	Avg. DB Length, µm	Avg. No. of fragments	Avg. TC Length, µm	Avg. DB Length, µm
4	17 (6)	8.2 (2)	16.3 (2.4)	10 (3)	7.3 (1)	14.2 (0.8)	7 (4)	5.9 (0.8)	18.6 (5.1)
5	46 (3)	12.1 (3.5)	20.1 (2.6)	32 (7)	9.8 (0.8)	22.5 (2.9)	25 (6)	7.8 (2.2)	20.4 (1.3)
6	55 (4)	18.7 (5.6)	31.6 (2.2)	43 (7)	12 (3.8)	26.4 (3.5)	36 (6)	9.5 (0.5)	19.2 (2.9)

TC – Transverse Matrix Crack; DB – Debond; Values given in parenthesis denotes standard deviation

Tab. 3

	Stress Transfer Length (STL)																			
System	**PB (mm)**				**PBTC (mm)**				**PBCC (mm)**				**DB (mm)**				**DBTC (mm)**			
Strain (%)	**EH**	**EL**	**PHY**	**PLY**	**EH**	**EL**	**PHY**	**PLY**	**EH**	**EL**	**PHY**	**PLY**	**EH**	**EL**	**PHY**	**PLY**	**EH**	**EL**	**PHY**	**PLY**
0.5	0.062	0.16	0.135	0.149	0.142	0.262	0.200	0.215	0.141	0.263	0.200	0.216	0.116	0.245	0.182	0.203	0.146	0.272	0.207	0.224
1	0.062	0.16	0.155	0.177	0.142	0.262	0.204	0.227	0.141	0.263	0.205	0.230	0.116	0.245	0.193	0.231	0.146	0.272	0.213	0.242
1.5	0.062	0.16	0.176	0.208	0.142	0.262	0.213	0.255	0.141	0.263	0.215	0.255	0.116	0.245	0.211	0.270	0.146	0.272	0.224	0.277
2	0.062	0.16	0.200	0.239	0.142	0.262	0.224	0.302	0.141	0.263	0.229	0.300	0.116	0.245	0.232	0.320	0.146	0.272	0.243	0.326

PB ─ Perfectly Bonded; PBTC ─ Perfectly Bonded with Transverse Matrix Crack; PBCC ─ Perfectly Bonded with Conical Matrix Crack; DB ─ Debonded; DBTC ─ Debonded with Transverse Matrix Crack

Tab.

Figure captions

Figure 1. (a) The loading arrangement for the fragmentation of a single embedded fibre composite **(b)** Birefringence pattern around an E-glass fibre-break under load at 4% strain.

Figure 2. Schematic drawing of the fibre/matrix cylinder and the region considered for FEA.

Figure 3. (a) Schematic illustration of the finite element model geometry used in the study (b) Drawing of deformed state of FEM with a conical matrix crack.

Figure 4. Fracture patterns at 6 % applied strain (a) Glass fibre in high modulus high yield strength matrix (PHY) with large transverse matrix crack and small conical matrix crack, (b) Fibre break in a short fragment resulting in small transverse crack and debonding (c) Glass fibre in medium modulus medium yield strength matrix (PMY) showing the increase in the length of conical crack, (d) Glass fibre in PMY resin showing asymmetrical transverse crack with a conical matrix crack (e) Glass fibre in low modulus low yield strength matrix (PLY) with two inclined conical matrix crack and small transverse matrix crack, (f) Glass fibre in PLY resin showing an undeveloped conical matrix crack on one side.

Figure 5. The effective stress transfer (EST) for glass fibre in different resin systems for a perfectly bonded fibre at different applied strains with (broken lines) and without (continuous lines) a transverse matrix crack.

Figure 6. The effective stress transfer (EST) for glass fibre in PHY resin system under different failure modes.

Figure 7. The effective stress transfer (EST) for glass fibre in PLY resin system under different failure modes.

Figure 8. The effective stress transfer (EST) for a glass fibre in EH resin system under different failure modes. (PB) A perfectly bonded fibre, (PBTC) Perfectly bonded fibre with a two fibre diameter-transverse matrix crack, (PBCC) Perfectly bonded fibre with two fibre diameter inclined-conical matrix crack, (DB) Two fibre diameter debond. (DBTC) Two fibre diameter-debond with transverse matrix crack.

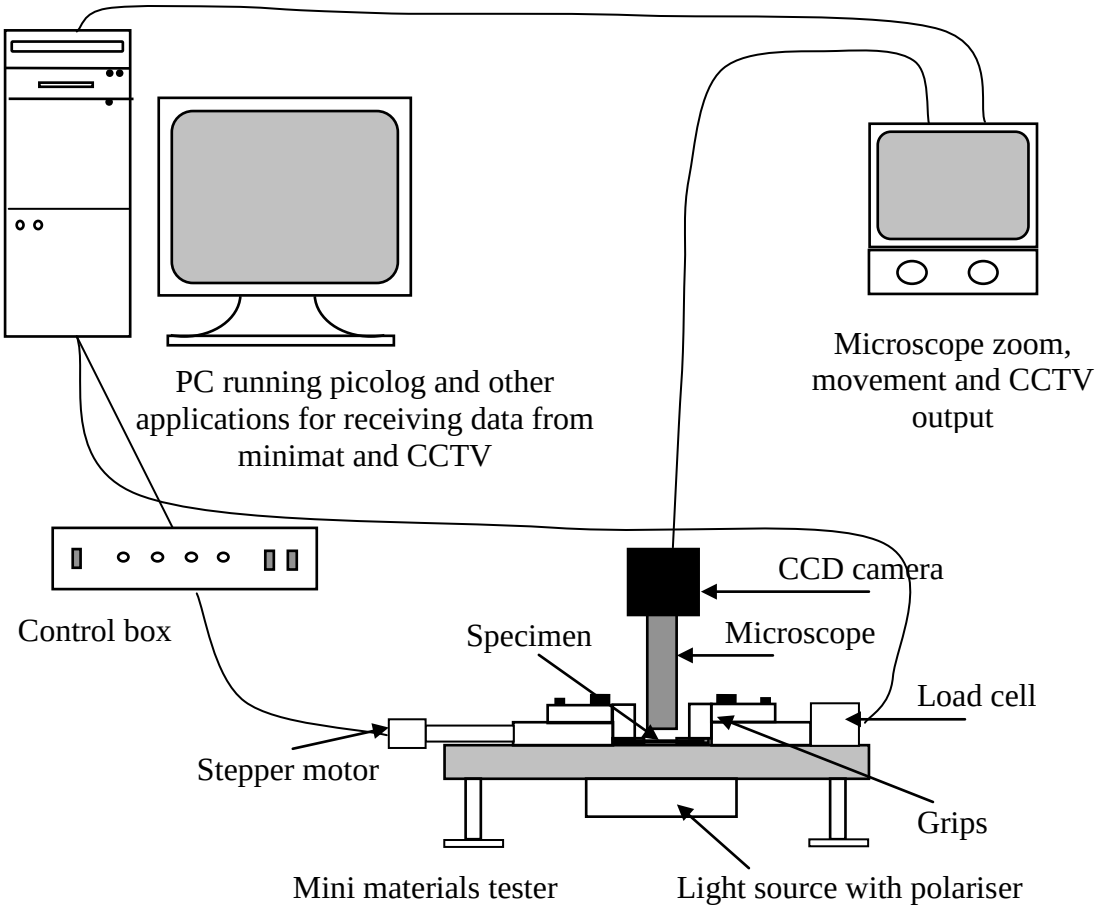
PC running picolog and other applications for receiving data from minimat and CCTV
Microscope zoom, movement and CCTV output
Control box
CCD camera
Specimen
Microscope
Load cell
Stepper motor
Grips
Mini materials tester
Light source with polariser

(a)

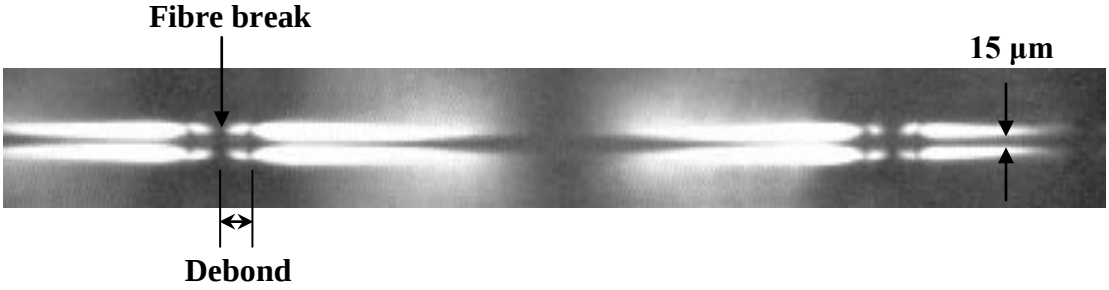
Fibre break
15 µm
Debond

(b)

Fig. 1 (a), (b)

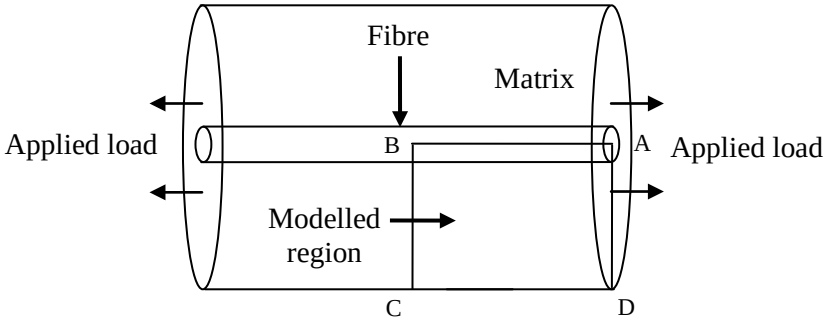
Fibre
Matrix
Applied load
B
A
Applied load
Modelled
region
C
D

Fig. 2

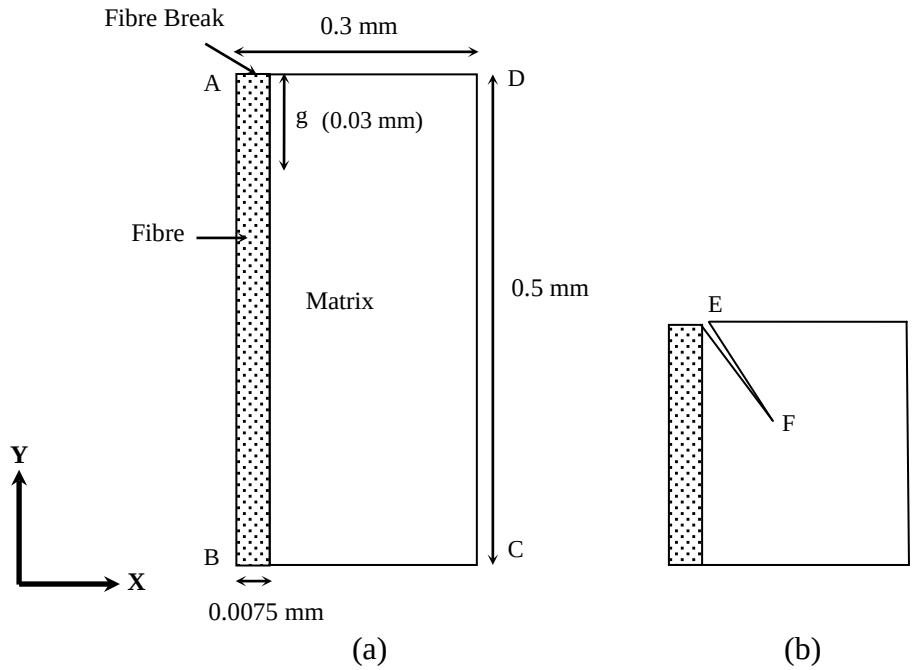
Fibre Break
0.3 mm
A
D
g (0.03 mm)
Fibre
Matrix
0.5 mm
E
F
Y
X
B
C
0.0075 mm
(a)
(b)

Fig. 3 (a), (b)

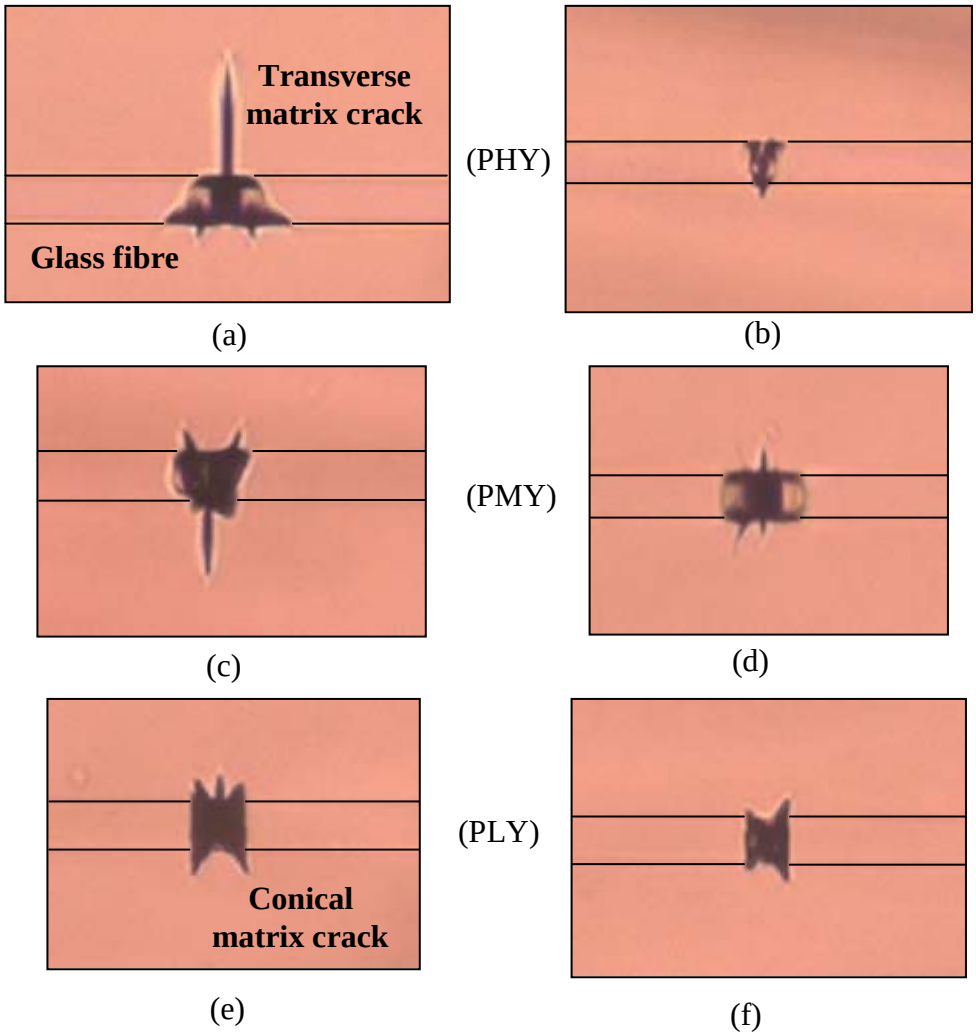
Transverse
matrix crack
Glass fibre
(PHY)
(a)
(b)
(PMY)
(c)
(d)
(PLY)
Conical
matrix crack
(e)
(f)

Fig. 4

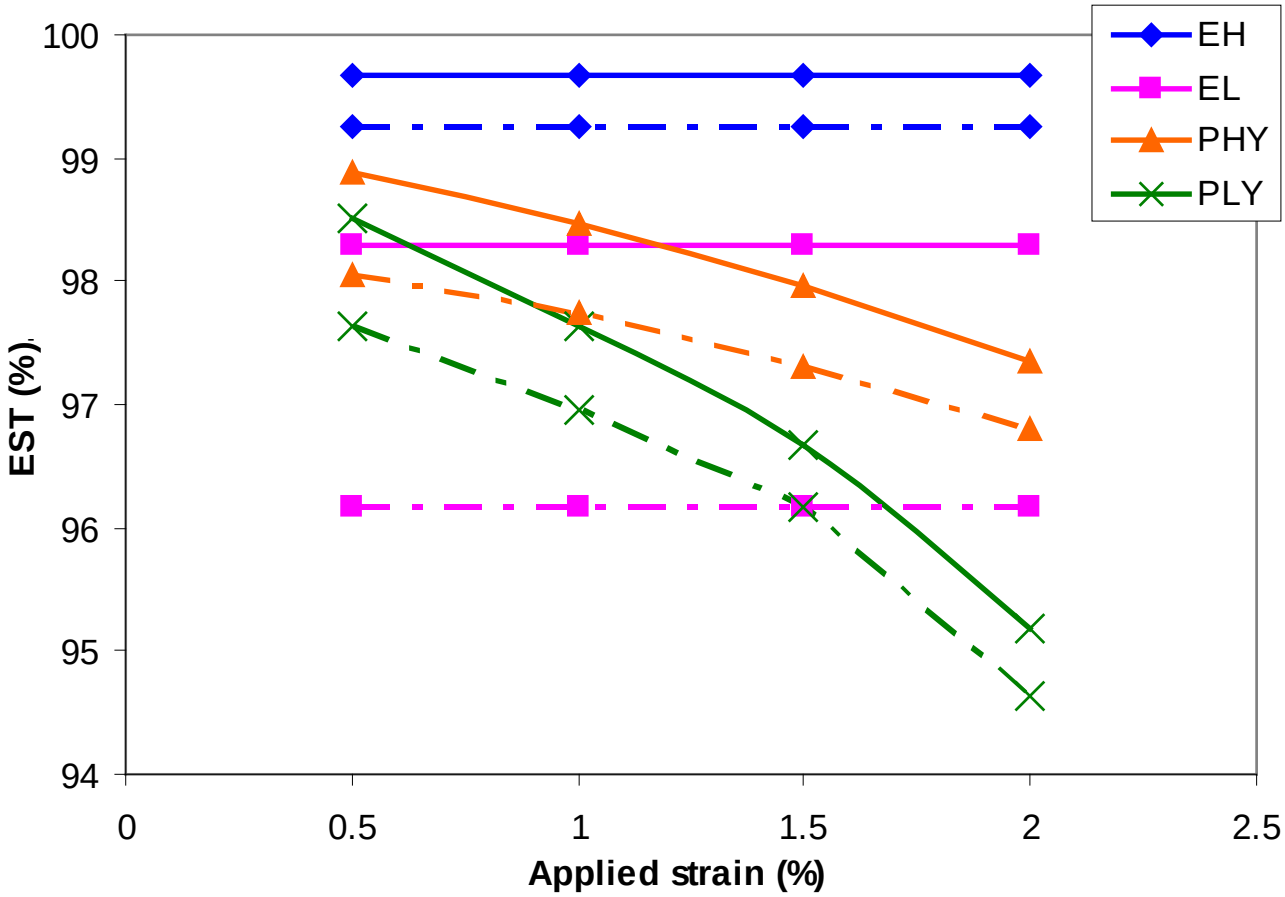
EH
EL
PHY
PLY
100
99
98
97
96
95
94
EST (%)
0
0.5
1
1.5
2
2.5
Applied strain (%)

Fig. 5

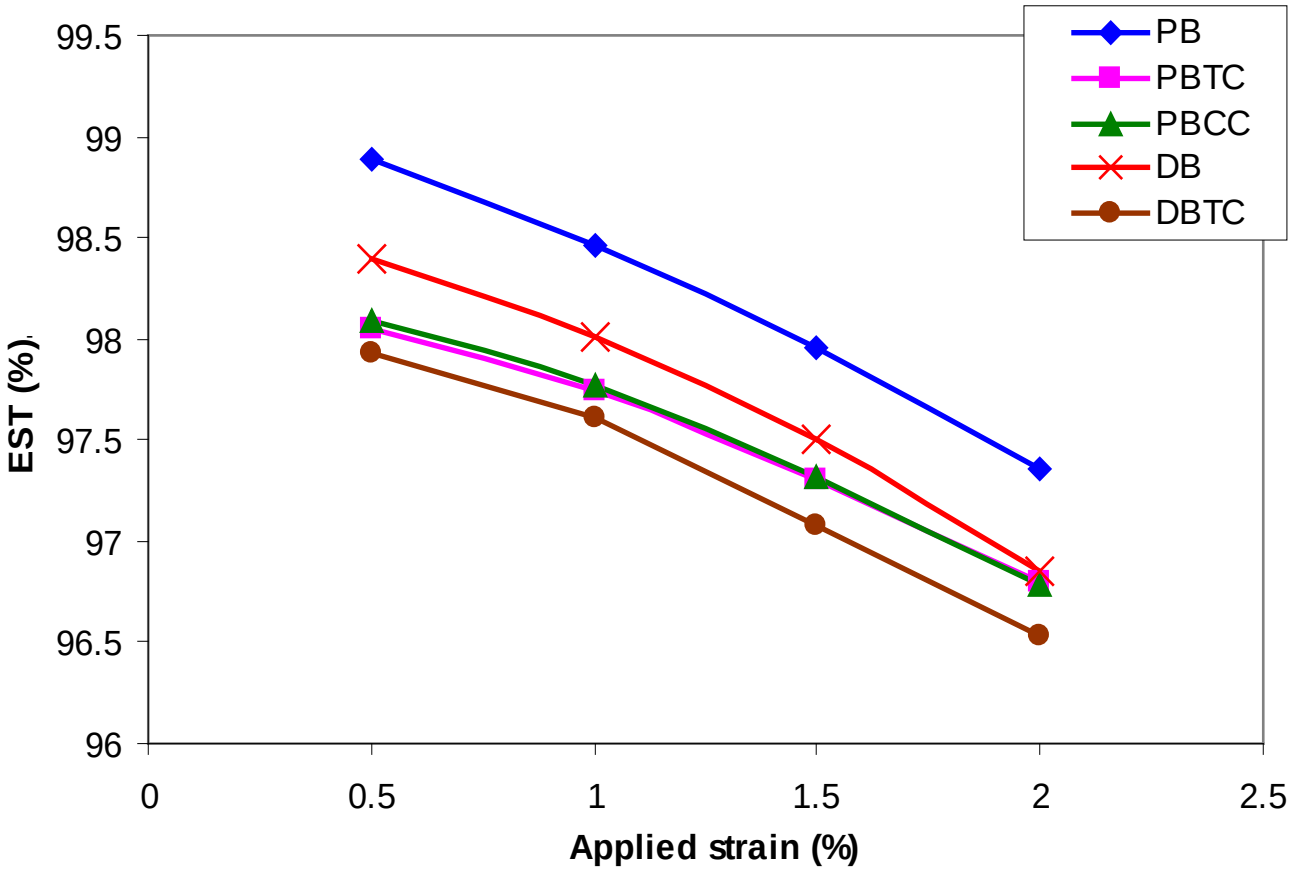
99.5
99
98.5
98
97.5
97
96.5
96
EST (%)
0
0.5
1
1.5
2
2.5
Applied strain (%)
PB
PBTC
PBCC
DB
DBTC

Fig. 6

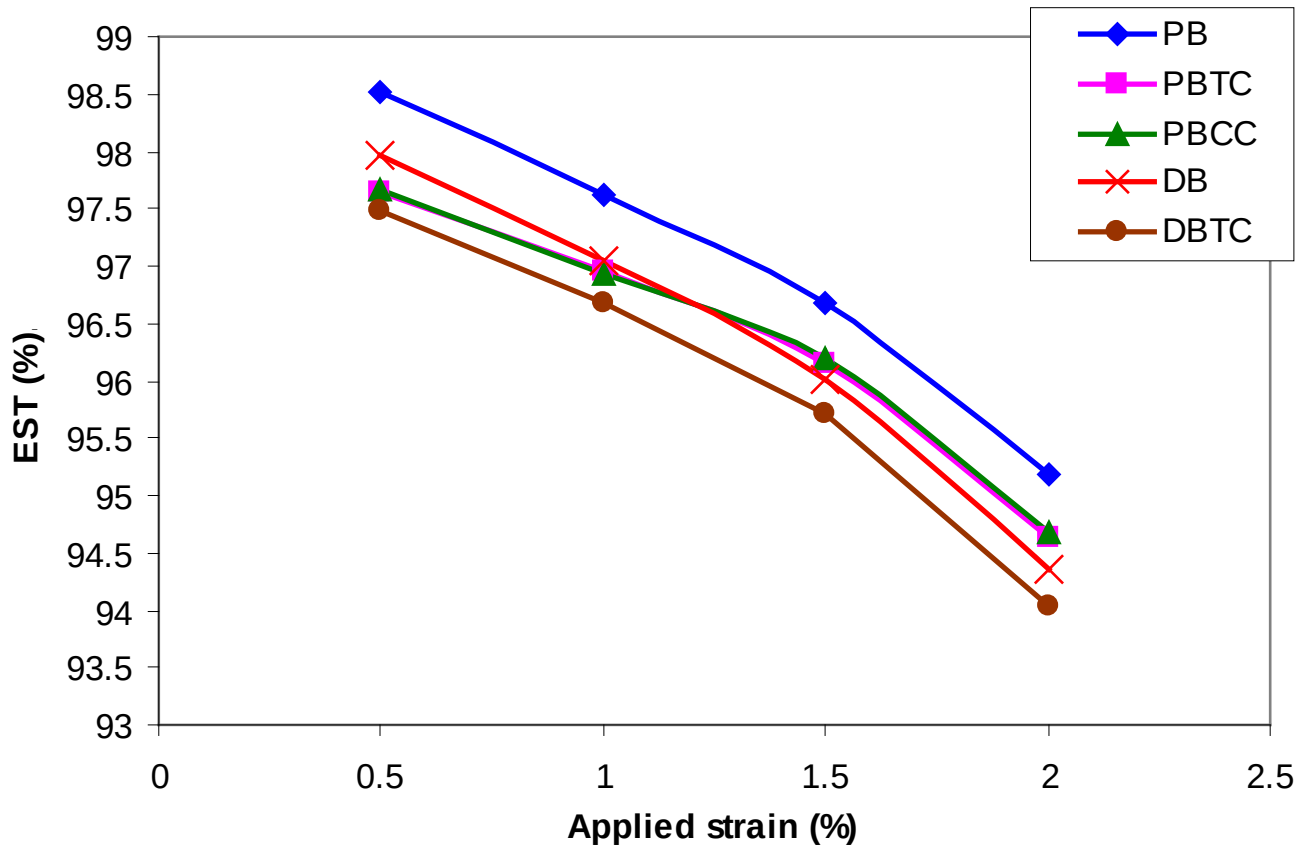
PB
PBTC
PBCC
DB
DBTC
EST (%)
99
98.5
98
97.5
97
96.5
96
95.5
95
94.5
94
93.5
93
0
0.5
1
1.5
2
2.5
Applied strain (%)

Fig. 7

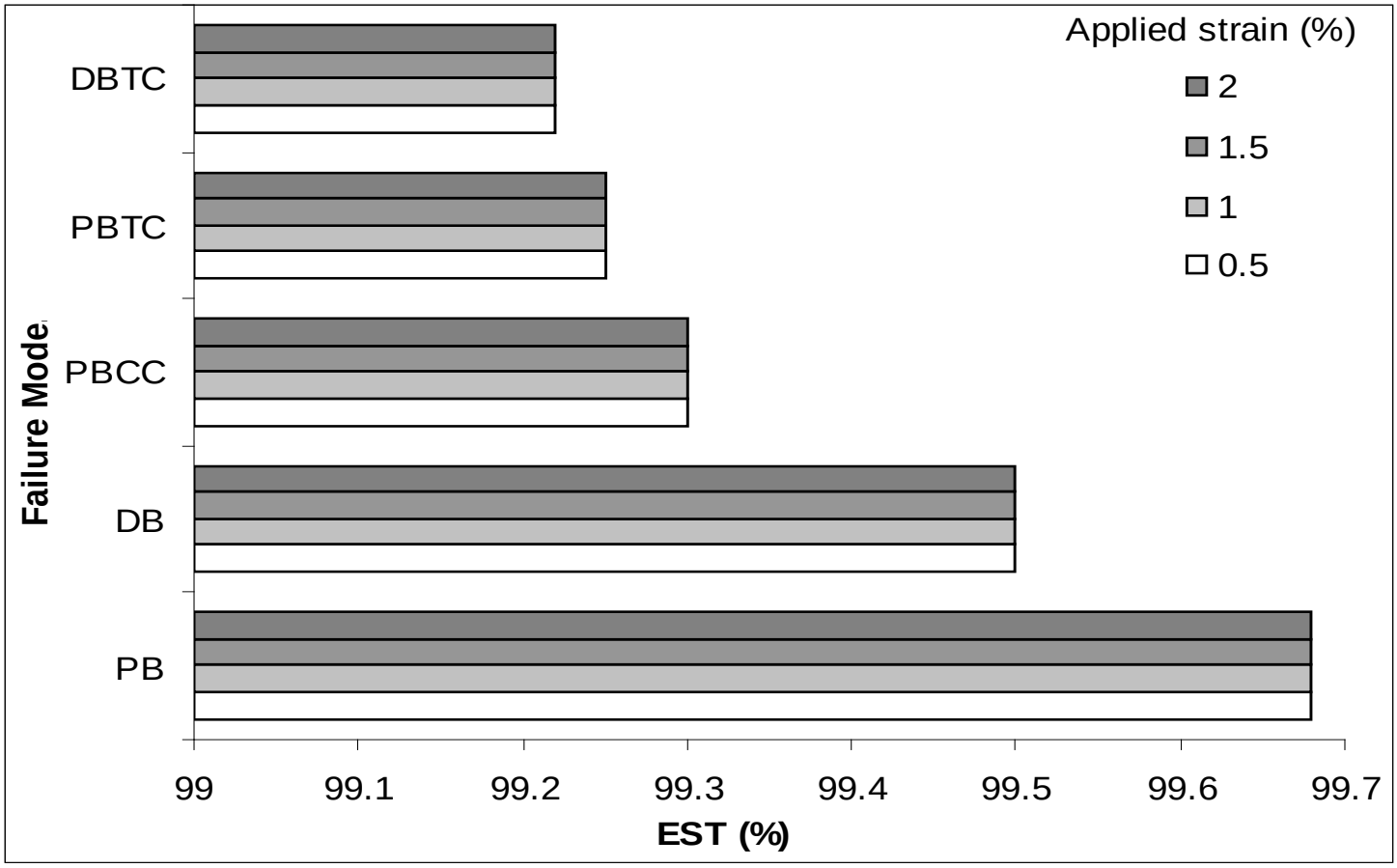
Applied strain (%)
2
1.5
1
0.5
DBTC
PBTC
PBCC
DB
PB
Failure Mode
99
99.1
99.2
99.3
99.4
99.5
99.6
99.7
EST (%)

Fig. 8